Available online at www.sciencedirect.com
SCIENCE DIRECT®
International Journal of Heat and Mass Transfer 47 (2004) 3097–3107
International Journal of HEAT and MASS TRANSFER
www.elsevier.com/locate/ijhmt

Role of surface structure in heterogeneous nucleation

Yusen Qi, James F. Klausner *, Renwei Mei

Department of Mechanical and Aerospace Engineering, University of Florida, P.O. Box 116300, Gainesville, FL 32611-6300, USA

Received 23 July 2003; received in revised form 23 February 2004
Available online 17 April 2004

Abstract

Nucleation site density measurements have been made for water on brass and stainless steel surfaces using a gas nucleation technique. It has been observed that nucleation sites are substantially more populated on the brass surface compared with the stainless steel surface. The difference is attributed to variations in the detailed surface structure. A vertical scanning interferometer has been used to gather statistical data on cavity mouth diameters and cavity half cone angles for the brass and stainless steel surfaces. The statistical data have been used to predict the nucleation site density, and satisfactory agreement is fortuitously obtained for the brass surface, while poor agreement is obtained for the stainless steel surface. Due to the large uncertainty in the probability of finding cavities that satisfy the gas trapping criteria, the statistical method does not appear to be useful for predicting nucleation site density on surfaces with randomly distributed cavities. It has been observed that only deep cavities are suitable for trapping vapor.

Keywords: Nucleation site density; Surface structure; Gas nucleation

1. Introduction

It is well known that the development of reliable mechanistic boiling models requires information on the nucleation site density. Therefore it has been the goal of researchers for the past 50 years to understand heterogeneous nucleation in boiling systems and develop correlations and models to predict its dependence on wall superheat, wettability, and surface structure. Corty and Foust [1] recognized that boiling takes place on surfaces with irregularities. They suggested that vapor trapped in these surface irregularities served as nucleation sites. This hypothesis was confirmed by Clark et al. [2] using micrographs of the heating surface. Gaertner and Westwater [3] measured the nucleation site density for a water and nickel-salt solution boiling on a copper surface. It was found that n/A is proportional to q_w^2, where n/A is the nucleation site density and q_w is the wall heat flux. Kurihara and Meyers [4] demonstrated that n/A is highly dependent on the roughness of the boiling surface.

An important breakthrough in quantitatively relating the heating surface microstructure to nucleation phenomena was made by Griffith and Wallis [5]. Using a conical geometry as an idealized surface cavity, they identified a minimum cavity mouth radius, r_c, required to generate vapor bubbles. They also demonstrated that for a specific surface–fluid combination the nucleation site density was correlated with the inverse of r_c at low heat flux. At higher heat flux the correlation appeared to break down. Others who have correlated nucleation site density with the critical cavity radius include Mikic and Rohsenow [6], Lorenz et al. [7], Bier et al. [8], Eddington and Kenning [9], Barthau [10], and Luke and Runowski [11]. Cornwell [12] conducted a very detailed study of the geometry of naturally formed nucleation site cavities in pool boiling. In general, the cavity sizes of actual sites tend to be slightly smaller than r_c. Hsu [13] accounted for the liquid thermal boundary layer surrounding a static vapor embryo using a conduction analysis in pool boiling and suggested there exists both a minimum and maximum cavity radius which will permit the incipience of vapor bubbles. Zeng and Klausner [14] measured

* Corresponding author. Tel.: +1-352-392-3506; fax: +1-352-392-1071.
E-mail address: klaus@ufl.edu (J.F. Klausner).

0017-9310/$ - see front matter © 2004 Elsevier Ltd. All rights reserved.
doi:10.1016/j.ijheatmasstransfer.2004.02.019

Nomenclature

d	cavity diameter, μm
$f(d)$	probability density function for finding cavities with diameter d, μm^{-1}
$g(\beta)$	probability density function for finding cavities with half cone angle β, rad^{-1}
h	height of the gas/liquid interface above the cavity, μm
H	distance between peaks, μm
n/A	nucleation site density, cm^{-2}
N/A	number of cavities per unit area, cm^{-2}
r_c	critical cavity radius, μm
Greek symbols	
β	half cone angle, rad
Δp	change in pressurization, MPa
μ_d	mean of the cavity diameter distribution, μm
θ	liquid solid contact angle, rad
σ	liquid/gas interfacial surface tension, N/m
σ_d	standard deviation of the cavity diameter distribution, μm

nucleation site density in flow boiling. Their data were re-analyzed by Thorncroft et al. [15], and it was demonstrated that both the maximum and minimum cavity radii are important in flow boiling nucleation.

It has been well known that only cavities that contain vapor or gas can serve as nucleation sites for heterogeneous boiling. Bankoff [16] was the first to establish a criterion for cavities capable of trapping vapor. Using conical cavities as the model, Bankoff proposed that the liquid solid contact angle, θ, must be greater than twice the half cone angle, β, for cavities to trap gas or vapor; i.e. $\theta > 2\beta$. More recently, Wang and Dhir [17] extended the vapor-trapping criterion to include conical, spherical, and sinusoidal cavities.

Tong et al. [18] demonstrated that the presence on non-condensable gas as well as contact angle hysteresis can exert a large influence on the incipience point of vapor bubbles in pool boiling systems. The contact angle hysteresis has a large impact on highly wetting fluids. Cornwell and Schuller [19] also reported on the effects of contact angle hysteresis on incipience.

Messina and Park [20] studied pool boiling heat transfer from surfaces in which a precise array of pits was formed on the heating surface using chemical etching. It was found that the pit density on the heating surface has a profound influence on the boiling curve. An increasing pit density enhances the rate of heat transfer. It was also noted that extremely shallow or jagged pits were substantially more efficient for nucleation than well-formed pits. Luke [21] concluded that a single roughness parameter cannot account for the effect of surface structure on boiling heat transfer. Luke and Gorenflo [22] showed that different heating surfaces with the same mean roughness can have very different heat transfer characteristics, depending on the surface preparation. Benjamin and Balakrishnan [23] demonstrated that nucleation site density does not increase monotonically with the average roughness. Luke et al. [24] used an ultrasonic stylus system to record detailed information on the surface microstructure. In order to identify potential vapor trapping cavities from the three-dimensional surface microstructure, a rolling ball technique was proposed.

Yang and Kim [25] suggested that the nucleation site density for a given surface may be computed from knowing the size distribution of cavities, the distribution of the cavity half cone angles, the minimum cavity mouth radius required for nucleation, and the liquid/solid contact angle. A scanning electron microscope was used to analyze the surface microstructure. Yang and Kim compared three nucleation site density data points for pool boiling of water on a mirror-finished stainless steel heating surface with those computed, and the data appear to agree well. Yet the maximum superheat tested was 2.6 °C. Wang and Dhir [17,26] also proposed a statistical method for predicting nucleation site density based on surface microstructure. A copper surface was well polished and surface cavities were viewed with an optical microscope. The cavity mouth size distribution and surface wettability were considered for spherical cavities. Many data were considered with varying wettability conditions, and the nucleation site density data agreed with the predicted data to within ±60%.

The main shortcomings of the statistical models noted above are: (1) they do not allow for interference from adjacent sites and (2) the critical radius is calculated based on a mean wall superheat, when in reality the wall superheat for heterogeneous nucleate boiling surfaces experiences substantial temporal and spatial variations. Kenning and Del Valle [27] argued that as the heating surface becomes increasingly populated with nucleation sites, adjacent sites may thermally interfere with one another. Calka and Judd [28] found that existing nucleation sites tend to activate adjacent sites that are within a distance of a bubble diameter and inhibit the formation of sites that are at a distance greater than a departure diameter and within three departure diameters of the active site. No influence of the active site was noted at a distance greater than three departure diameters. Golobic et al. [29] and Kenning and Yan [30]

used liquid crystal thermography to demonstrate that large spatial and temporal variations of wall superheat are characteristic of boiling surfaces and thermal interference between adjacent nucleation sites occurs even at low heat fluxes. The most recent studies by Wienecke et al. [31] of a single active nucleation site on a vertical plate in pool boiling, showed that unlike the horizontal pool boiling case, successive bubbles did not always activate at the same local superheat. The variability increased with increasing heat flux. It was suggested that the observed behavior could not be explained in terms of time-averaged temperature gradients at the wall. These data cast doubt as to whether each cavity on a surface has a unique critical radius required for nucleation. Pasamehmetoglu et al. [32,33] and Sadasivan et al. [34] developed a large-scale computer simulation that explored the interactions between hundreds of randomly distributed nucleation sites. This multi-cell model demonstrated the importance of transient conduction and resultant thermal interaction among nucleation sites, which could lead to non-linear behavior.

In this work extensive gas nucleation experiments have been carried through on copper and stainless steel surfaces that were prepared using fine grit sandpaper. Nucleation site density measurements have been made for a change in pressurization up to 3 atmospheres. Detailed measurements of the surface microstructure have been made using a vertical scanning interferometer. Distributions for cavity sizes and half cone angles have been identified and a statistical model has been used to predict the resulting nucleation site density. The objectives of the current work are to (1) investigate the usefulness of statistical models to predict nucleation site density on commercial surfaces, (2) develop criteria for identifying potential cavities from topography data on commercial surfaces, and (3) develop a robust methodology for constructing surface structure statistical distributions useful in predicting nucleation site density.

Gas nucleation studies have been previously reported by Brown [35] and Eddington et al. [36]. When comparing nucleation site density measured as a function of the critical cavity radius by gas nucleation with those measured during nucleate boiling, the comparison was not satisfactory. However, Kenning [37] re-analyzed the data of Eddington et al. by accounting for the non-linear variation of the saturation pressure with temperature and found improved agreement. Yet the nucleation site density measured during gas nucleation experiments tends to be greater than that measured for nucleate boiling experiments with the same critical cavity mouth radius. The advantage of using gas nucleation experiments to examine the performance of statistical models is that the possibility of thermal interference between adjacent nucleation sites is eliminated.

2. Experimental facility

A gas nucleation facility, shown in Fig. 1, was designed and fabricated for the present experiments. The

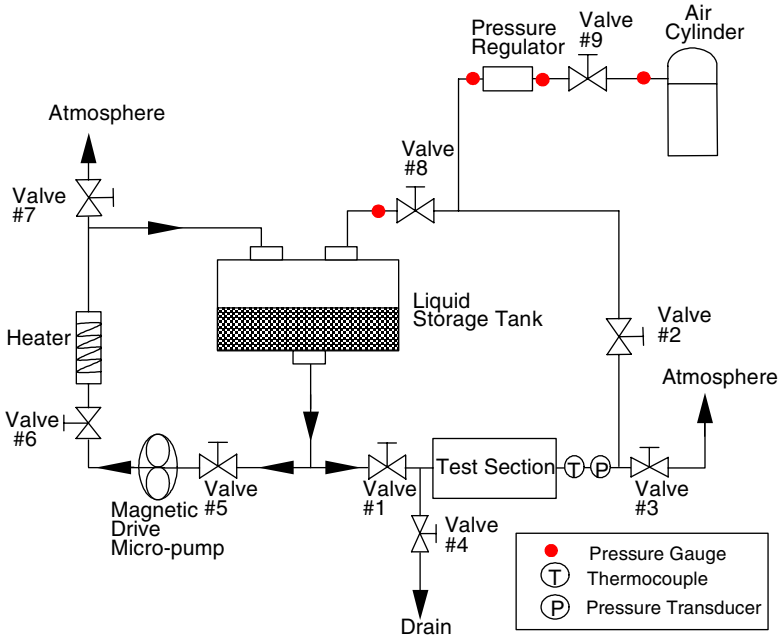

Fig. 1. Schematic diagram of the gas nucleation facility.

operation of the facility is similar to that used by Eddington et al. [36]. The 20 liter liquid storage tank is half filled with water. Valves 5, 6, 8, and 9 are opened and a portion of the facility is pressurized with a charged air cylinder, and the degree of pressurization is controlled with a pressure regulator. Valve 9 is closed, and a variable speed magnetically driven micro-pump is used to circulate pressurized water through the liquid storage tank. As water is sprayed into the liquid storage tank, it gradually becomes saturated with air. The water is allowed to circulate for 40 min to insure that it becomes fully saturated with dissolved air. With valves 3 and 4 closed, valve 2 is opened and then valve 1 is opened in sequence. By adjusting the valves in the sequence described allows the test section to equilibrate to the same pressure as the liquid storage tank. Water from the storage tank fills the test section while dissolved gas remains in solution. The pressure and temperature of the water in the test section are recorded. Valves 1 and 2 are closed and valve 3 is opened, which de-pressurizes the test section. The resulting temperature and pressure are recorded again. As the test section is depressurized, nucleation sites form on the test surface, which is photographed with a high-resolution digital camera from a side view, as shown in Fig. 2. Using back lighting, each bubble directs the light toward the camera lens, and each individual bubble is identified by its bright spot.

The test section is fabricated from 19 mm thick polycarbonate with an inner cross section of 30.48 mm wide by 17.4 mm high. It has a circular recess in which a 25.4 mm diameter metallic sample may be inserted. The test section is flanged to allow it to connect with the experimental facility. For the present investigation brass and stainless steel surfaces have been investigated. The surface is prepared by first polishing it with 120 grit sandpaper. A 400 grit silicon carbide sandpaper is used to put a final finish on the surface. Prior to inserting the metallic disk into the test section it is thoroughly cleaned with ethyl alcohol. The maximum pressure the test section can accommodate is 3 bars.

The nucleating gas bubbles on the test surface are photographed with a Videk Megaplus digital camera that has 1320×1035 pixel resolution. Sigmascan image processing software is used to assist in identifying nucleation sites from the digital image. The pressure in the test section is measured with a Viatran strain gauge type pressure transducer. The temperature is measured with a single type E thermocouple. An Access 12 bit digital data acquisition facility is used to record the pressure and temperature measurements. The uncertainty of the pressure measurement is ±0.2 kPa and the uncertainty of the temperature measurement is ±0.5 °C. At low nucleation site density, the measurement of n/A is exact. At higher nucleation site density the measurement uncertainty is approximately ±2%.

3. Nucleation site density measurements

Nucleation site density measurements, n/A, have been made on the brass and stainless steel surfaces over a pressure range of 1.2–3 bars. A total of 53 measurements have been made for the brass surface and 44 measurements for the stainless steel surface. According to classical heterogeneous nucleation theory, a gas bubble will nucleate from a conical cavity when the cavity mouth radius is greater than the critical cavity radius given by

$$r_c = \frac{2\sigma}{\Delta p}, \tag{1}$$

where σ is the liquid/gas interfacial surface tension and Δp is the change in pressurization in the test section. Fig. 3a shows the variation of nucleation site density with $\frac{\Delta p}{2\sigma}$ for the brass surface while Fig. 3b shows that for the stainless steel surface. It is observed that the nucleation

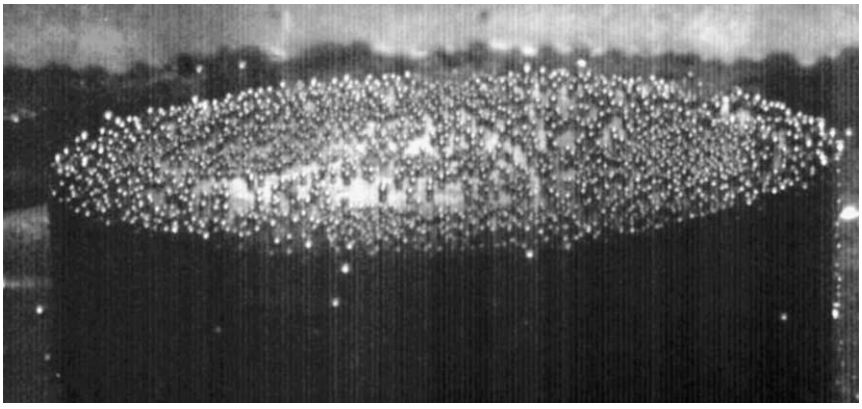

Fig. 2. A typical image of gas nucleation sites on the test surface.

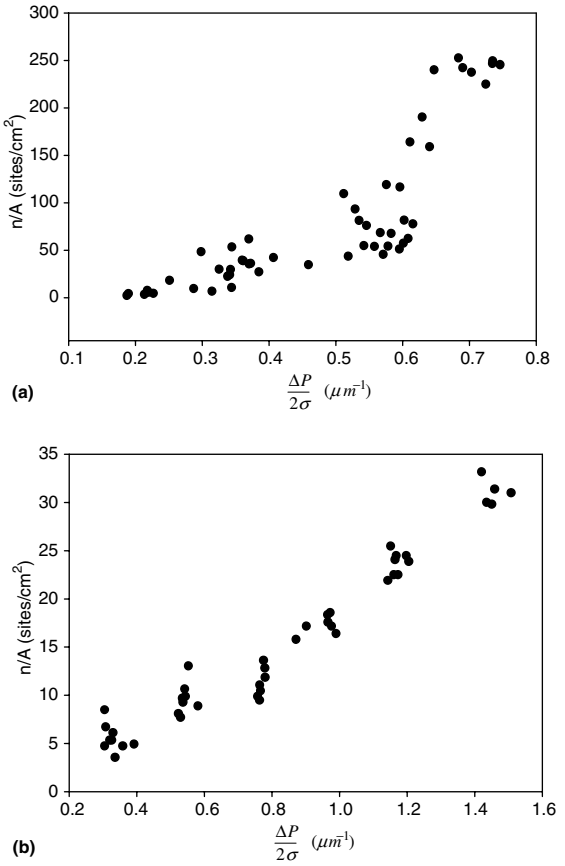

Fig. 3. (a) Variation of nucleation site density with $\frac{\Delta P}{2\sigma}$ for brass surface and (b) variation of nucleation site density with $\frac{\Delta P}{2\sigma}$ for stainless steel surface.

site density for the brass surface increases very rapidly with increasing $\frac{\Delta p}{2\sigma}$. Furthermore, the brass surface is observed to be very populated with gas bubbles. The nucleation site density reaches as high as 250 sites/cm^2. In contrast, the nucleation site density for the stainless steel surface does not increase as rapidly with $\frac{\Delta p}{2\sigma}$, and the largest nucleation site density observed over the pressure range considered is approximately 34 sites/cm^2. It is also observed that for the same change in pressurization, the measured n/A are scattered. The data for the brass are more scattered than those for the stainless steel.

The static liquid/solid contact angle measured between the water and the stainless steel for an ensemble of 14 trials is 1.35 rad (77.4°) with a standard deviation of 0.07 rad (4.2°). The static/liquid solid contact angle between the water and brass for an ensemble of 13 trials is 1.27 rad (73.1°) with a standard deviation of 0.06 rad (3.7°). The water is slightly more wetting on brass than on stainless steel, although the degree of wettability on both surfaces is quite similar. This result indicates that the very different nucleation behavior on stainless steel and brass must be due to differences in surface structure and not wettability.

4. Surface characterization

In order to characterize the surface structure, a Wyko NT1000 vertical scanning interferometer (VSI) manufactured by Veeco Metrology Group is used. The surface area covered by a single scan depends on the lens objective utilized. For the analysis of the brass surface an area of 595×453 μm is typically covered. The VSI will scan the surface and store the three dimensional location of every point on the surface with a resolution of approximately 0.1 nm. The rms roughness of the stainless steel surface is 0.88 μm, while that of the brass is 1.02 μm. The brass surface is rougher than the stainless steel, but this difference alone cannot account for the substantial difference in n/A between the two surfaces. With the three dimensional topography data, it is desired to identify gas trapping cavities on the surface. After much deliberation it was concluded that a unique algorithm for identifying gas trapping cavities from the three dimensional data is not feasible due to the highly irregular topography. As an alternative, it was decided to analyze two dimensional cross-sections of the surface. For the current work, the brass and stainless steel surfaces have been fully analyzed.

4.1. Identifying gas trapping cavities

A typical x–z profile of the surface is shown in Fig. 4, where z is in the direction of the surface depth. This scan shows the relative change in surface height along the x-direction. The length of the scan in the x-direction is 301 μm. Typically 22 x–z profiles separated by a distance of 20 μm are considered for each spot on the brass surface analyzed. The analysis of the brass surface

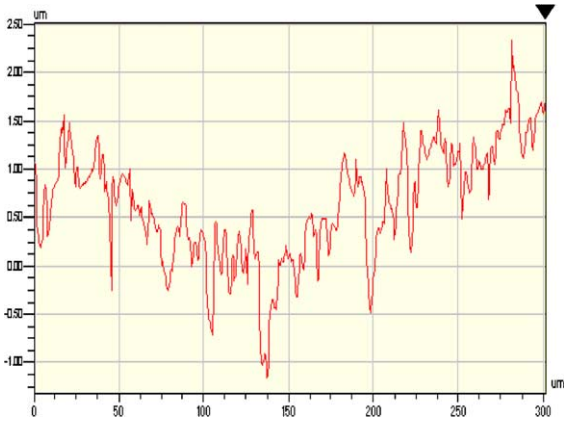

Fig. 4. Typical x–z surface profile using VSI.

considers data collected from 3 randomly selected spots for a total of 66 x–z profiles. It is assumed that the statistical distribution of cavities on the surface is homogeneous since a uniform surface polishing technique was used along the entire surface.

In order to identify gas trapping cavities the following procedure is implemented. Every peak in the x–z profile is identified. There exists a cavity on either side of the peak. In order to find the characteristic diameter associated with the cavity, a horizontal line is extended from the peak until it intersects the sidewall of a higher peak. The length of the extended horizontal line is taken to be the characteristic cavity diameter. It is important to note that the VSI is not capable of identifying re-entrant type cavities.

An uncertainty arises when cavities are located within cavities as shown in Fig. 5a. The two possibilities are that A and B serve as separate gas trapping cavities with respective diameters of d_A and d_B or cavities A and B are merged to behave as a single gas trapping cavity C with diameter d_C. The following arguments are used to resolve this uncertainty. As the nucleating surface is flooded, the single merged cavity C will trap gas, provided cavities A and B are recessed far enough into C and C has a sufficiently small half cone angle, β, so that it does not flood. A gas/liquid interface will form over C as shown in Fig. 5b. Due to pressure fluctuations in the bulk liquid that exist during the nucleating process the liquid vapor interface may be deformed as shown in Fig. 5c. As the pressure wave passes, the gas/liquid interface will recover to a static position as shown in Fig. 5b and cavity C will be preserved as a gas trapping cavity. If cavities A and B are not sufficiently recessed in C, a pressure fluctuation can cause the gas/liquid interface to deform as shown in Fig. 5d. After the pressure wave passes, the gas liquid interface will recover to a static position as shown in Fig. 5e, in which gas cavities A and B will serve as the vapor trapping cavities.

In order to determine which outcome is more probable a cavity with a static gas/liquid interface is shown in Fig. 6 with a uniform radius of curvature, r. The cavity is dimensioned as follows: diameter, d; half cone angle, β; and liquid solid contact angle, θ. From geometrical considerations, the height of the gas/liquid interface above the cavity, h, is given by

$$h = \frac{d}{2}\tan\left[\frac{\pi/2 - \theta + \beta}{2}\right]. \tag{2}$$

Given that H is the distance between peaks that form cavity C and cavities A and B as shown in Fig. 5a, the postulated criterion to determine the most probable potential gas trapping cavities is: a single merged cavity C is most probable, as shown in Fig. 5b, when $h < H$, otherwise recessed cavities A and B are most probable as shown in Fig. 5e.

Using this criterion to identify the most probable potential gas trapping cavities, a computer code was developed to automate the process of identifying cavity mouth diameters and half cone angles from the x–z

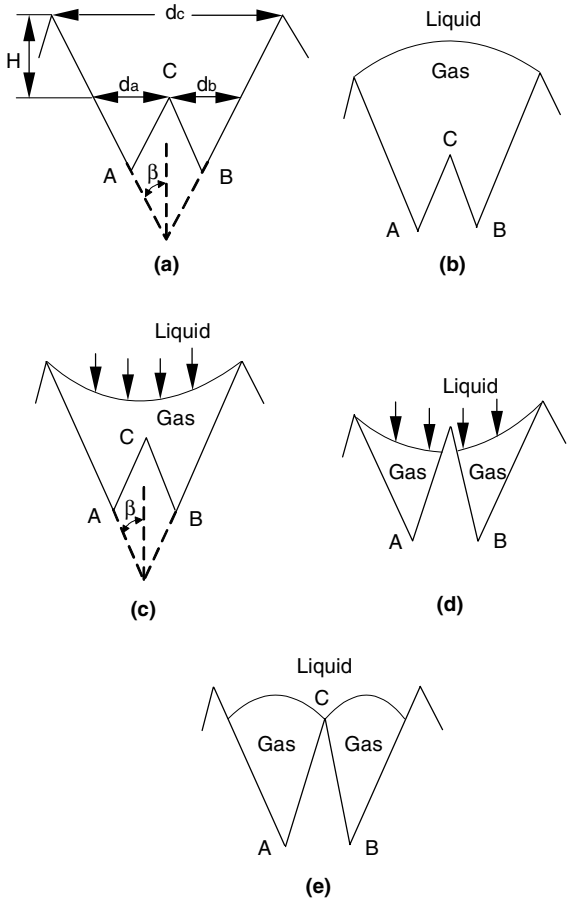

Fig. 5. Different gas/liquid interface configurations for cavities residing inside a cavity.

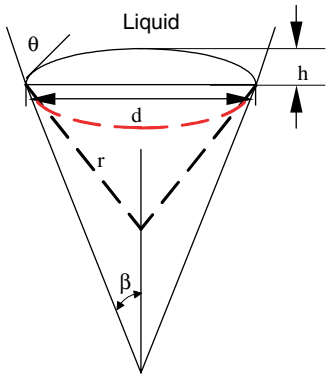

Fig. 6. Cavity dimension with gas/liquid interface at cavity mouth.

surface profiles obtained using the VSI. Sixty-six profiles are examined for the brass surface and a total of 6025 cavities were identified with an associated cavity mouth radius and half cone angle. For the stainless steel surface 77 profiles are examined and a total of 6704 cavities were identified. After examining the data, it is readily apparent that most of the cavities are shallow and will be flooded according to Bankoff's gas trapping criterion: cavities will trap gas or vapor when $\theta > 2\beta$. In fact, finding a cavity that does satisfy Bankoff's gas trapping criterion is a very low probability event.

The prediction of the nucleation site density requires information on the statistical distribution of cavity mouth diameters and cavity half cone angles. In order to better resolve the distribution with cavities that are more likely to trap gas, a filtering procedure was applied. The ratio of the cavity depth to mouth diameter was identified for each cavity, and the mean and standard deviation were determined. Only those cavities in which the ratio of the cavity depth to mouth diameter is greater than the mean plus one standard deviation are used to construct cavity diameter and half cone angle distributions. After filtering, only 1412 cavities remain out of the original 6025 cavities originally identified on the brass surface and 1039 cavities remain for the stainless steel surface.

4.2. Distribution of surface cavities

After filtering the surface cavity data as described, the probability density function for finding a cavity within a specified size range was computed for the brass surface over an interval of 0.28 μm with the remaining cavity size data. It was found that the best fit to the majority of size distribution data follows a Weibull distribution of the form

$$f(d) = \frac{\lambda}{\omega}\left(\frac{d}{\omega}\right)^{\lambda-1}\exp\left[-\left(\frac{d}{\omega}\right)^{\lambda}\right];$$
$$d \geqslant 0; \quad \omega, \lambda > 0, \tag{3}$$

where d is the cavity diameter and λ and ω are related to the mean and standard deviation. The parameters λ and ω are related to the mean and standard deviation by

$$\omega = \frac{\mu_{\mathrm{d}}}{\Gamma\left(1+\frac{1}{\lambda}\right)} \tag{4}$$

and

$$\lambda = \ln\left[\omega^{2\lambda} - \frac{\sigma_{\mathrm{d}}^2 + \mu_{\mathrm{d}}^2}{\Gamma\left(1+\frac{2}{\lambda}\right)}\right], \tag{5}$$

where μ_{d} is the mean of the distribution and σ_{d} is the standard deviation. From the measured distribution of cavity sizes the mean cavity diameter, denoted as $\mu_{\mathrm{d,meas}}$, and the standard deviation, denoted as $\sigma_{\mathrm{d,meas}}$, are found. Here, $\mu_{\mathrm{d,meas}} = 4.72$ μm, $\sigma_{\mathrm{d,meas}} = 3.9$ μm for brass surface; $\mu_{\mathrm{d,meas}} = 2.68$ μm, $\sigma_{\mathrm{d,meas}} = 1.79$ μm for stainless steel surface. With the exception of a couple of data points, the Weibull distribution fits the data reasonably well as shown in Fig. 7a and b. It is observed that the cavity mouths on the stainless steel surface are statistically smaller than those on the brass surface, which partially accounts for the smaller nucleation site density on the stainless steel surface compared with the brass.

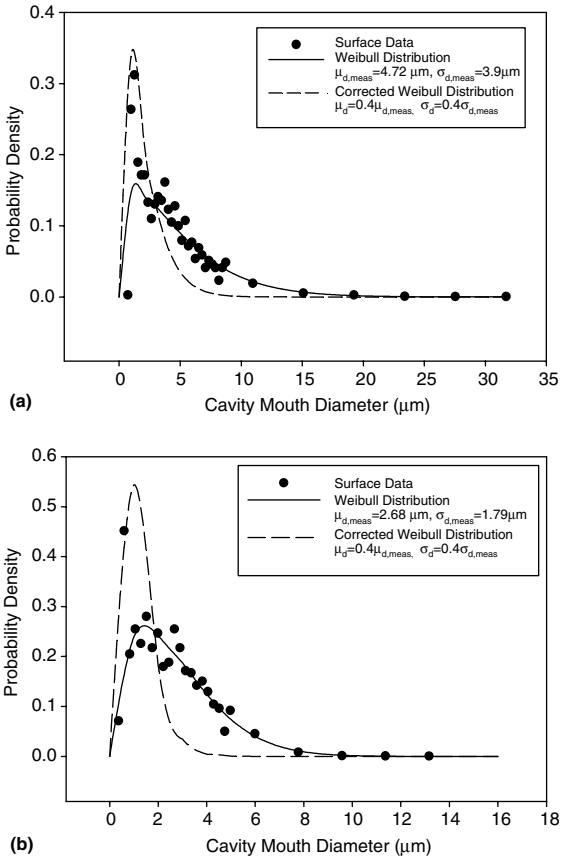

Fig. 7. (a) Cavity mouth diameter distributions for brass surface and (b) cavity mouth diameter distributions for stainless steel surface.

4.3. Distribution of cavity half cone angles

Of the remaining cavity data, it was found that the probability density distribution of cavity half cone angles are best represented with the function

$$g(\beta) = \frac{A\left(\frac{\pi}{2}-\beta\right)^2}{B + \left(\frac{\pi}{2}-\beta\right)^6}, \tag{6}$$

where $A = 0.01913$ and $B = 0.0001$ for the brass surface while $A = 0.091$ and $B = 0.0023$ for the stainless steel

surface. Fig. 8a shows the probability density distribution of cavity half cone angles for the brass surface compared with Eq. (6), while Fig. 8b shows the same data on a log-log scale. Fig. 9a and b show similar trends for the stainless steel surface. It is of significant interest to note at smaller cavity half cone angles, $g(\beta)$ follows the scaling law $(\frac{\pi}{2}-\beta)^{-4}$. This behavior is indicative that the cavity geometry has a fractal nature. It is also particularly noteworthy that finding cavities with smaller half cone-angles is a very low probability event.

Following Bankoff's gas trapping criterion, on the brass surface only cavities with half cone angles less than $\beta = 0.635$ rad can serve as nucleation sites since the liquid/solid contact angle for water on brass was measured to be $\theta = 1.27$ rad. To satisfy the gas trapping criterion on the stainless steel surface, the half cone angle must be less than $\beta = 0.675$ since the liquid/solid contact angle $\theta = 1.35$. It is observed from Figs. 10 and 11 that finding a cavity that satisfies the gas trapping criterion is a very low probability event. In fact, it has been observed that only very deep cavities satisfy the vapor-trapping criterion. This may give some insight as to why rougher surfaces tend to produce more nucleation sites.

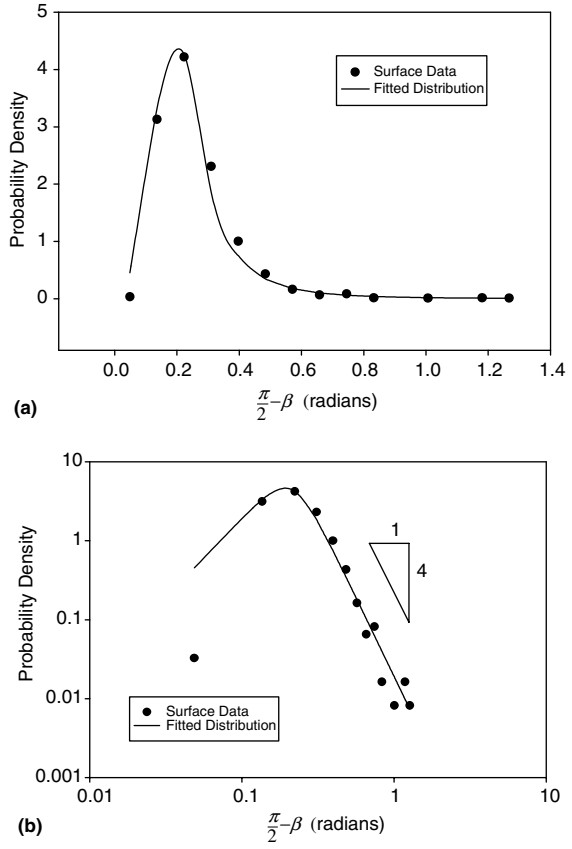

Fig. 8. (a) Cavity half cone angle distribution for brass surface using the linear scale and (b) cavity half cone angle distribution for brass surface using the log–log scale.

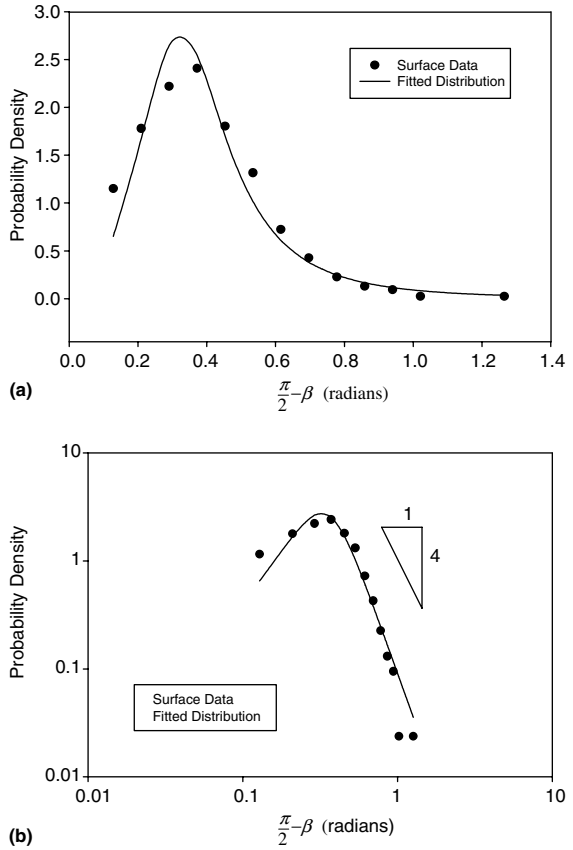

Fig. 9. (a) Cavity half cone angle distribution for stainless steel surface using the linear scale and (b) Cavity half cone angle distribution for stainless steel surface using the log–log scale.

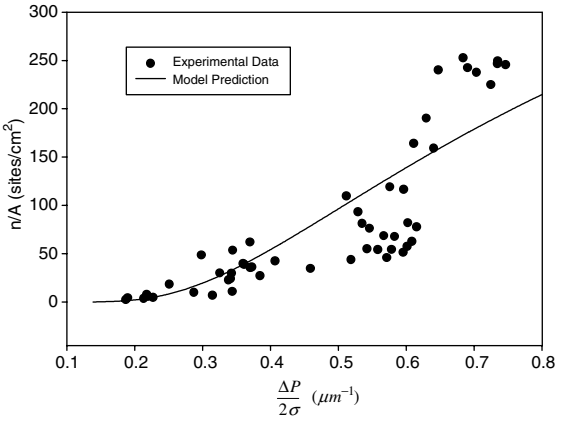

Fig. 10. Comparison between measured and predicted nucleation site density on brass surface.

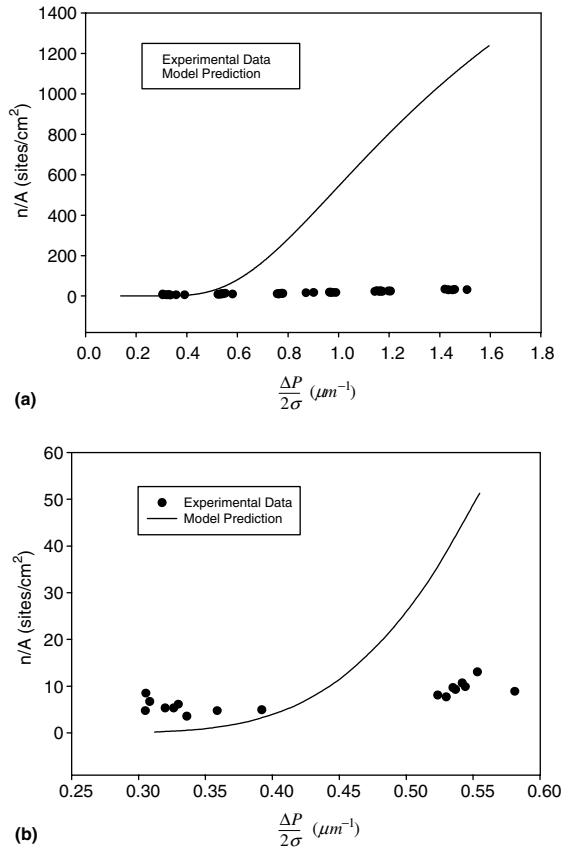

Fig. 11. (a) Comparison between measured and predicted nucleation site density on stainless steel surface and (b) Comparison between measured and predicted nucleation site density on stainless steel surface within low pressure change range.

5. Prediction of nucleation site density

Here the statistical method is used to predict nucleation site density. Following Yang and Kim [25] an estimation of the nucleation site density is given by

$$\frac{n}{A} = \frac{N}{A}\int_{2r_c}^{\infty} f_{3D}(d)\,\mathrm{d}d \int_0^{\theta/2} g(\beta)\,\mathrm{d}\beta, \tag{7}$$

where $\frac{N}{A}$ is the number of cavities per unit area and r_c is evaluated from Eq. (1). Although it has been assumed that the cavity mouths are circular in shape, it is recognized that their shape is likely to be non-uniform. Therefore, the identification of cavity diameters from a two-dimensional profile is biased. In determining the parameters ω and λ for the Weibull distribution using Eqs. (4) and (5) the measured mean cavity mouth diameter and standard deviation are corrected. $f_{3D}(d)$ is modified from Eq. (3) by using $\mu_d = C\mu_{d,meas}$ and $\sigma_d = C\sigma_{d,meas}$ in Eqs. (4) and (5) where $C = 0.4$ is an empirical correction. The modified distribution, f_{3D}, is also shown in Fig. 7a and b. For the 1412 brass cavities, $\frac{N}{A} = 2.1 \times 10^5$ cavities/cm^2, and $\frac{N}{A} = 2.37 \times 10^5$ cavities/cm^2 for the stainless steel cavities. The last integral in Eq. (7) represents the probability of finding a cavity with $\beta < \theta/2$. As mentioned earlier, this is a very low probability event, and the degree of accuracy to be expected from a fitted distribution at such low probability is poor. Therefore, the last integral in Eq. (7) is replaced by the measured probability $P(\beta < \theta/2)$ even though it also has large statistical uncertainty. $P(\beta < \theta/2)$ is 0.0028 for the brass surface and 0.012 for the stainless steel surface.

Combining Eqs. (3) and (7) the estimated nucleation site density variation with $\frac{\Delta p}{2\sigma}$ for the brass and stainless steel surfaces are respectively shown in Figs. 10, 11a and b. There are several observations worthy of discussion. The first is that the apparently good agreement for the brass surface is purely fortuitous. As seen in Fig. 11a and b there is considerable error between the predicted and measured $\frac{n}{A}$ on the stainless steel surface. The cause of this error is the very large statistical uncertainty associated with the probability of finding gas trapping cavities. One approach to reducing the statistical uncertainty is to increase the sample size by several orders of magnitude. The main drawback with this approach is that it would be restrictively laborious. As it is, many hours of labor were required just to obtain the current sample size.

A basic premise in using the statistical method for predicting nucleation site density is that the statistical distribution of cavities on the surface is homogeneous. While this appears to be valid for the distribution of cavity mouth diameters and half cone angles in general, the distribution of cavity half cone angle that actually trap vapor appears to be inhomogeneous. This is likely the reason nucleation sites are non-uniformly distributed on the nucleating surface.

These findings suggest that the statistical method for predicting nucleation site density on commercial heat transfer surfaces with randomly distributed cavities is not likely to be accurate using the current state-of-the-art in surface metrology technology. However, the qualitative trends predicted by the model are supported by the data. The model may be useful in designing specially prepared surfaces that promote high nucleation site density and heat transfer.

6. Concluding remarks

The nucleation site densities on stainless steel and brass surfaces have been measured using the gas nucleation method. Although the same sandpaper polishing method is used to prepare both surfaces, very different behavior is observed. The difference is attributed to the difference in surface structure. A methodology has been presented that allows the identification of surface cavities

based on a two-dimensional surface scan. This includes cavities residing inside cavities. Using the detailed surface analysis, a framework has been presented for predicting nucleation site density. The distribution of cavity half cone angle shows that the probability of finding vapor trapping cavities on a commercially prepared metal surface is very low. Since the probability in finding vapor trapping cavities is low and the statistical uncertainty is large, accurate quantitative prediction of nucleation site density using statistical models is difficult. The order of magnitude difference in nucleation site density between the brass and stainless steel surface has not been adequately addressed by this study. Some of the difference is attributable to the smaller cavity sizes on the stainless steel. However, most of the difference is likely due to the brass having a larger population of vapor trapping cavities, yet this cannot be confirmed since the data on $P(\beta < \theta/2)$ are unreliable.

Past studies of surface structure and nucleation site density have not focused on the difficulty in identifying cavities that actually trap vapor. In fact, the detailed surface analysis provided by this study suggests that only deep cavities are vapor trapping ones. This is contrary to the suggestion by Messina and Park [20] that shallow pits are more efficient for nucleation site formation. The distribution of cavity half cone angles suggests their formation is of a fractal nature. The fractal nature of the cavity geometry may have some utility in predicting the occurrence of vapor trapping cavities. This is an area open for further research.

Ongoing work will focus on using the gas nucleation method to test the statistical model with precisely manufactured cavities. It will also involve determining whether gas nucleation experiments are useful in predicting nucleation site density in nucleate boiling, where large temporal and spatial temperature variations are common.

Acknowledgements

Financial support for this work was partly funded by NASA Glenn Research Center under contract NAG3-2750.

References

[1] C. Corty, A. Foust, Surface variables in nucleate boiling, Chem. Eng. Prog. Symp. Ser. 17 (51) (1955) 1–12.
[2] H.B. Clark, P.S. Strenge, J.W. Westwater, Active sites for nucleate boiling, Chem. Eng. Prog. Symp. Ser. 55 (29) (1959) 103–110.
[3] R.F. Gaertner, J.W. Westwater, Population of active sites in nucleate boiling heat transfer, Chem. Eng. Prog. Symp. Ser. 56 (30) (1960) 39–48.
[4] H.M. Kurihara, J.E. Meyers, The effects of superheat and surface roughness on boiling coefficients, AIChE J. 6 (1) (1960) 83–91.
[5] P. Griffith, J.D. Wallis, The role of surface conditions in nucleate boiling, Chemical Eng. Progr. Symp. Ser. 56 (30) (1960) 49–63.
[6] B.B. Mikic, W.M. Rohsenow, A new correlation of pool-boiling data including the effect of heating surface characteristics, Trans. ASME Ser. C, J. Heat Transfer 91 (2) (1969) 245–250.
[7] J.J. Lorenz, B.B. Mikic, W.M. Rohsenow, Effect of surface conditions on boiling characteristics, in: Proceedings of the 5th International Heat Transfer Conference, Tokyo, 1974.
[8] K. Bier, D. Gorenflo, M.I. Salem, Y.M. Tanes, Pool boiling heat transfer and size of active nucleation centers for horizontal plates with different roughness, in: Proceedings of the 6th International Heat Transfer Conference, Toronto, vol. 1, 1978, 151–156.
[9] R.I. Eddington, D.B.R. Kenning, The prediction of flow boiling bubble populations from gas bubble nucleation experiments, in: Proceedings of the 6th International Heat Transfer Conference, vol. 1, 1978, pp. 275–280.
[10] G. Barthau, Active nucleation site density and pool boiling heat transfer—an experimental study, Int. J. Heat Mass Transfer 35 (2) (1992) 271–278.
[11] A. Luke, T. Runowski, Heat transfer and size distribution of active nucleation sites in boiling of hydrocarbons, in: Proceedings of the International Conference on Convective Flow and Pool Boiling, Irsee, Engineering Foundation Publication, 1997.
[12] K. Cornwell, Naturally formed boiling site cavities, Lett. Heat Mass Transfer 4 (1977) 63–72.
[13] Y.Y. Hsu, On the size range of active nucleation cavities on a heating surface, J. Heat Transfer 98c (1962) 207–216.
[14] L.Z. Zeng, J.F. Klausner, Nucleation site density in forced convection boiling, J. Heat Transfer 115 (1993) 215–221.
[15] G.E. Thorncroft, J.F. Klausner, R. Mei, Suppression of flow boiling nucleation, J. Heat Transfer 119 (1997) 517–524.
[16] S.G. Bankoff, Entrainment of gas in the spreading of liquid over a rough surface, AIChE J. 4 (1) (1958) 24–26.
[17] C.H. Wang, V.K. Dhir, Effect of surface wettability on active nucleation site density during pool boiling of saturated water, J. Heat Transfer 115 (1993) 659–669.
[18] W. Tong, A. Bar-Cohen, T.W. Simon, S.M. You, Contact angle effects on boiling incipience of highly-wetting liquids, Int. J. Heat Mass Transfer 33 (1) (1990) 91–103.
[19] K. Cornwell, R.B. Schuller, A study of boiling outside a tube bundle using high speed photography, Int. J. Heat Mass Transfer 25 (5) (1982) 683–690.
[20] A.D. Messina, E.L. Park, Effects of precise arrays of pits on nucleate boiling, Int. J. Heat Transfer 24 (1981) 141–145.
[21] A. Luke, Pool boiling heat transfer from horizontal tubes with different surface roughness, Int. J. Refrig. 20 (8) (1997) 561–574.
[22] A. Luke, D. Gorenflo, Nucleate boiling heat transfer of HFCs and HCs in heat pump application: state of the art

and new developments, in: Proceedings of the 6th IEA Heat Pump Conference, Berlin, 1999.
[23] R.J. Benjamin, A.R. Balakrishnan, Nucleation site density in pool boiling of saturated pure liquids: effect of surface microroughness and surface and liquid physical properties, Exp. Therm. Fluid Sci. 15 (1997) 32–42.
[24] A. Luke, D. Gorenflo, Heat transfer and size distribution of active nucleation sites in boiling propane outside a tube, Int. J. Therm. Sci. 39 (2000) 919–930.
[25] S.R. Yang, R.H. Kim, A mathematical model of the pool boiling nucleation site density in terms of the surface characteristics, Int. J. Heat Mass Transfer 31 (6) (1988) 1127–1135.
[26] C.H. Wang, V.K. Dhir, On the gas entrapment and nucleation site density during pool boiling of saturated water, J. Heat Transfer 115 (1993) 670–679.
[27] D.B.R. Kenning, V.H. Del Valle, Fully-developed nucleate boiling: overlap of areas of influence and interference between bubble sites, Int. J. Heat Mass Transfer 24 (6) (1981) 1025–1032.
[28] A. Calka, R.L. Judd, Some aspects of the interaction among nucleation sites during saturated nucleate boiling, Int. J. Heat Mass Transfer 28 (12) (1985) 2331–2342.
[29] I. Golobic, E. Pavlovic, S. Strgar, D.B.R. Kenning, Y.Y. Yan, Wall temperature variations during bubble growth on a thin plate: computations and experimentations, Eurothermal Seminar no. 48, Paderborn, ETS, Pisa, 1996, pp. 25–32.
[30] D.B.R. Kenning, Y.Y. Yan, Pool boiling heat transfer on a thin plate: features revealed by liquid crystal thermography, Int. J. Heat Mass Transfer 39 (1996) 3117–3137.
[31] M. Wienecke, Y.Y. Yan, D.B.R. Kenning, Bubble nucleation and growth during saturated pool boiling on thin vertical plate, in: M. Lehner, D. Mewes, U. Dinglreiter, R. Tauscher (Eds.), Applied Optical Measurements, Springer-Verlag, Berlin, 1999, pp. 107–120.
[32] K.O. Pasamehmetoglu, R.A. Nelson, Cavity-to-cavity interaction in nucleate boiling: the effect of heat conduction within the heater, AIChE Symp. Ser. 87 (283) (1991) 342–351.
[33] K.O. Pasamehmetoglu, P.R. Chappidi, C. Unal, R.A. Nelson, Saturated pool nucleate boiling mechanisms at high heat fluxes, Int. J. Heat Mass Transfer 36 (1993) 3859–3868.
[34] P. Sadasivan, C. Unal, R.A. Nelson, Nonlinear aspects of high heat flux nucleate boiling heat transfer, J. Heat Transfer 117 (1995) 981–989.
[35] W.T. Brown, Study of flow surface boiling, Ph.D. Thesis, Department of Mechanical Engineering, Massachusetts Institute of Technology, 1967.
[36] R.I Eddington, D.B.R. Kenning, A.I. Korneichev, Comparison of gas and vapor bubble nucleation on a brass surface in water, Int. J. Heat Mass Transfer 21 (1978) 855–862.
[37] D.B.R. Kenning, Experimental methods: looking closely at bubble nucleation, Engineering Foundation Conference Boiling 2000, Keynote Lecture, 2000.